Free Electron Attachment and Rydberg Electron Transfer to NF_3 Molecules and Clusters

Nike Ruckhaberle, Lars Lehmann, Stefan Matejcik,† and Eugen Illenberger*

Institut für Physikalische und Theoretische Chemie, Freie Universität Berlin, Takustr. 3, D-14195 Berlin, Germany

Yves Bouteiller, Veronique Periquet, Luc Museur, Charles Desfrançois, and Jean-Pierre Schermann

Laboratoire de Physique des Lasers, Institut Galilée Université Paris-Nord, F-93430 Villetaneuse, France

Received: July 24, 1997; In Final Form: October 10, 1997[⊗]

Free electron attachment in the energy range 0−10 eV and Rydberg electron transfer (RET) to NF_3 molecules, NF_3 clusters, and NF_3/Ar clusters are studied by means of negative ion mass spectrometry. The experimental results are compared with density functional theory (DFT) calculations. In the free electron experiment gas-phase NF_3 generates the dissociative attachment (DA) products F^-, F_2^-, and NF_2^- appearing from a broad resonance around 2 eV, in agreement with an earlier beam experiment. The most abundant fragment, F^-, exhibits a small "threshold" signal at incident energies close to 0 eV. This signal increases with the target gas temperature and is due to transitions from the neutral to the anion involving vibrationally excited states close to the intersection between the two potential energy surfaces. From the temperature dependence of this threshold signal the activation energy for the exothermic DA reaction $e^- + NF_3 \rightarrow F^- + NF_2$ is derived as $E_a = 0.1 \pm 0.05$ eV. Time-of-flight (TOF) analysis reveals that F^- arises from a repulsive electronic state releasing the fragments with appreciable kinetic energy. Free electron attachment and RET to NF_3 clusters produce undissociated cluster ions $(NF_3)_n^-$ including the monomer. In the case of free electrons they are still dominantly formed via the 2 eV resonance followed by intracluster relaxation processes. DFT calculations predict a lowering of the symmetry from C_{3v} to C_s on going from the neutral to the anion with one F atom substantially enlarged from the NF_2 plane. The calculated (adiabatic) electron affinities are $EA(NF_3) = 1.71$ eV and $EA(NF_2) = 1.18$ eV. From the appearance energy in the DA experiment we derive $EA(NF_2) = 1.1 \pm 0.1$ eV.

Introduction

NF_3 is frequently used as a fluoride source in ion−molecule experiments,[1] in gas laser media,[2] and also in connection to dry etching[3−5] for the production of very large-scale integrated (VLSI) circuits. It is one of the few F-containing molecules yielding copious amounts of F^- in discharge plasmas. NF_3-containing plasmas have the ability to remove native oxide from silicon wafers. In addition, the use of NF_3 prevents carbon contamination and creates only minor crystal damages.

Although NF_3 is a well-known electron scavenger, so far only dissociative attachment (DA) has been observed either in low-pressure[6] or in high-pressure[7] mass spectrometric studies.

The most abundant ion is F^- appearing from a resonance near 2 eV.[6] It is due to the DA reaction

$$e^- + NF_3 \rightarrow NF_2 + F^- \qquad (1)$$

which has an energy threshold of −0.9 eV.

To our knowledge, no observation of NF_3^- in the gas phase and no value for the electron affinity of NF_3 were reported in the literature so far.

In this contribution we study the following.

(a) Attachment of free electrons in the range 0−5 eV to NF_3 with considerably improved energy resolution with respect to previous beam experiments.[6] The kinetic energy release of F^- in reaction 1 is determined by means of a time-of-flight (TOF) analysis. In addition, from the temperature dependence of the relative F^- DA cross section the activation energy of reaction 1 can be derived.

(b) Free electron attachment to NF_3 clusters yielding the stabilized monomeric parent anion NF_3^- and the larger homologues $(NF_3)_n^-$.

(c) Electron transfer in the collision of Rydberg excited Xe atoms with mixed NF_3/Ar clusters also yielding the undissociated compounds $(NF_3)_n^-$, $n = 1, 2, ...$, and complexes of the form $(NF_3^-)\cdot Ar_n$, $n = 1, 2, ...$

(d) Density functional theory (DFT) calculations on NF_3^- and the dissociation channels observed in the experiment. These calculations show that the anion NF_3^- is very far from the C_{3v} geometry of the neutral NF_3.

Experimental Section

A. Free Electron Attachment to NF_3 and NF_3 Clusters. *Relative Cross Section Curves for Dissociative Attachment (DA) and Associative Attachment (AA).* Electron attachment to single NF_3 molecules and clusters is studied in the Berlin laboratory by means of two different crossed beam setups, an effusive beam apparatus[8] and a supersonic beam apparatus,[9] both equipped with a mass spectrometric detection system. The effusive beam contains single molecules under collision-free conditions and the supersonic jet a distribution of clusters. In both cases the molecular beams are crossed at a right angle with the electron beam.

† Alexander von Humboldt Research Fellow. Permanent address: Institute of Plasmaphysics, Comenius University, Bratislave, Slovakia.

⊗ Abstract published in *Advance ACS Abstracts,* November 15, 1997.

S1089-5639(97)02422-5 CCC: $14.00

The electron beam is generated by a trochoidal electron monochromator (TEM),[11] which uses a combination of a magnetic and an electric field. In that configuration the electrons emitted from a hot filament are spatially dispersed according to their velocity. Since the magnetic field (∼100 G) is present over the entire monochromator, it further acts as a guiding field for the energy-selected electrons and aligns them toward the collision region. The TEM has proven to be particularly suitable for studying electron attachment reactions, since the axial magnetic field prevents spreading of the beam at low energies so that reasonable intensities (∼30 nA) can be achieved to very low energies, i.e., close to 0 eV.

For the present experiments the energy resolution was below 0.1 eV. The energy scale is calibrated by the well-known standards SF_6[12] or CCl_4.[13]

The "effusive" molecular beam containing single molecules is formed by effusing NF_3 gas through a 0.5 mm hole from a small heatable cylinder directly connected to the reaction chamber. Inside the cylinder the molecules undergo many collisions with the walls, thus reaching thermal equilibrium before entering the reaction chamber. Within the heated reaction volume we can assume that the gas density varies as $n \propto T^{-1/2}$ (molecular flow conditions). The count rate in the figures are *not* corrected for this effect.

The supersonic beam is formed by adiabatic expansion of an NF_3/Ar mixture at several bars through an 80 μm nozzle. The beam then passes a skimmer (800 μm), which separates the expansion chamber from the main chamber where the molecular beam is crossed with the electron beam.

In both setups, negative ions created in the interaction region defined by the crossing of the electron beam with the molecular beam are extracted by a small electric field (<1 V cm^{-1}) and then accelerated toward the entrance hole of a commercial quadrupole mass filter. The mass-selected ions are detected by single-pulse counting techniques and recorded as a function of the incident electron energy.

TOF Analysis of Product Ions. Recording flight times of fragment ions on their way through the quadrupole to the detector offers a way to obtain information on the kinetic energy release in the decomposition of the corresponding transient negative ion (TNI).[14,15] For that reason the electron beam is pulsed (pulse width < 1 μs) and the flight time is recorded by means of time-to-amplitude conversion (TAC).

Under time-of-flight (TOF) conditions (ion draw out field now on the order of a few V cm^{-1}) the TOF spectrum consists of one peak having either a certain width or a more or less separated doublet, the latter signifying appreciable kinetic energy. A doublet arises when the aperture of the ion draw out configuration discriminates against fragment ions with initial velocity components perpendicular to the flight tube axis. The doublet is then due to ions emitted along the flight tube axis either directly toward the detector or away from it. The latter has to be reversed in the ion draw out field (E) and reach the detector with some time delay (ΔT) with respect to the former.

The kinetic energy release of the fragment ion of mass m_i is then given by

$$E_T(m_i) = \frac{(\Delta T q E)^2}{8 m_i} \qquad (2)$$

For a unimolecular decomposition yielding two fragments, the total translational energy (E_T) is then obtained from linear momentum conservation yielding

$$E_T = E_T(m_i)\frac{M}{m} \qquad (3)$$

where M is the mass of the parent molecule and m that of the neutral fragment.

B. Rydberg Electron Transfer to NF_3 Clusters. The Rydberg transfer experiments were performed in the Paris laboratory. The Rydberg electron-transfer method (RET) offers the possibility of investigating electron attachment in the thermal and subthermal range (3−300 meV) under well-controlled conditions. Electrons are initially bound in Rydberg atoms and transferred under single-collision conditions to molecular assemblies. Xenon atoms issued from a pulsed valve are first excited into metastable states by electron bombardment and further excited toward Rydberg nf states by means of a pulsed tunable dye laser (Coumarine 460, 480, or 500) pumped by an amplified YAG laser.[16] A beam of molecules or neutral clusters is produced by expanding a few tens of mbar of molecular NF_3 mixed with 3 bar of argon with a pulsed valve (General Valve, 0.15 mm nozzle). This beam passes downstream in a 2 mm conical nozzle and collides with the beam of Xe** atoms, which constitutes the ionization source. Ions are created by charge transfer from the Xe** atoms to the studied molecular systems and are extracted from the collision region by a low-voltage pulse delayed by 1 μs from the laser excitation shot. They are further accelerated in a TOF mass spectrometer and detected by a set of microchannel plates.

Results

A. Free Electron Attachment to NF_3. Figure 1 presents the relative DA cross sections for the different fragmentation channels. In agreement with the previous beam experiment[6] we observe the three fragments F^-, F_2^-, and NF_2^- appearing from a resonance feature around 2 eV. The appearance of these ions can be assigned to the following DA processes:

$$e^- + NF_3 \rightarrow NF_3^- \rightarrow F^- + NF_2\ (-0.93 \pm 0.02\ \text{eV}) \qquad (1a)$$

$$\rightarrow F + NF_2^- \qquad (1b)$$

$$\rightarrow F_2^- + NF\ (+0.9 \pm 0.4\ \text{eV}) \qquad (1c)$$

The numbers in parentheses refer to the thermodynamic limits (ΔH_o) calculated from $D(NF_2{-}F) = 2.47 \pm 0.04$ eV,[17] $\Delta H_f^{298}(NF_3) = -1.37 \pm 0.13$ eV,[18] $\Delta H_f^{298}(NF) = 2.6 \pm 0.3$ eV,[18] $EA(F) = 3.401$ eV,[19] and $EA(F_2) = 3.08 \pm 0.10$.[19]

The steep onset for NF_2^- formation suggests that channel 1b is accessible within the NF_3^- resonance energy; i.e., the experimentally observed appearance energy (AE) of NF_2^- corresponds to the energetic threshold (ΔH_o) of reaction 1b (see also Figure 7). Taking the present experimental result ($AE(NF_2^-) = 1.35 \pm 0.1$ eV), we obtain the electron affinity of the NF_2 radical as $EA(NF_2) = 1.1 \pm 0.1$ eV. The previously reported value was 1.68 ± 0.21 eV based on the considerably lower appearance energy ($AE(NF_2^-) = 0.9 \pm 0.1$ eV) derived in a beam experiment without an electron monochromator by unfolding the experimental data.[6] The stated accuracy in the appearance energy determination (±0.1 eV) was obviously much too optimistic in that experiment.

The exothermic DA channel 1a is associated with the release of considerable translational energy, as is obvious from the TOF experiments (Figure 2).

Figure 3 shows the result of the evaluation according to eqs 2 and 3, indicating that the fragments are released with an appreciable amount of translational energy. This suggests a

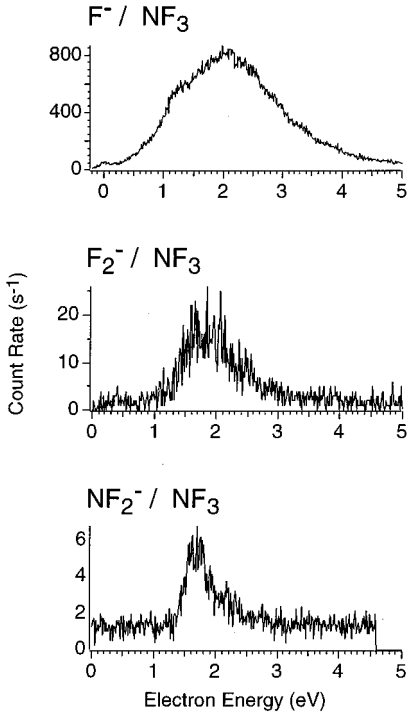

Figure 1. DA products observed in free electron attachment to NF_3 molecules.

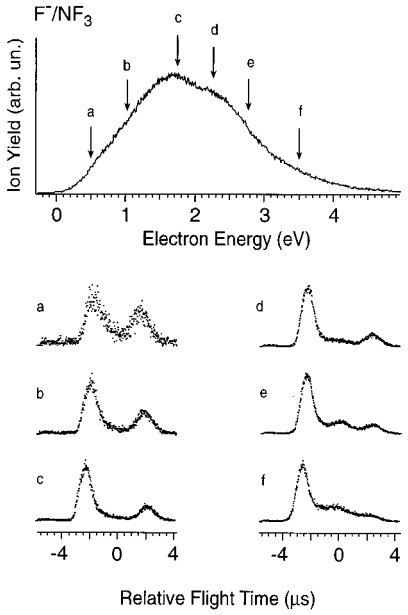

Figure 2. Time-of-flight spectra of F^- recorded at the indicated incident energies with a draw out field of 3 V cm^{-1}.

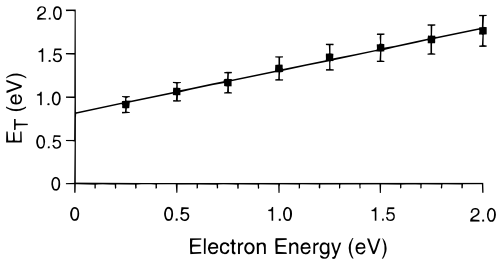

Figure 3. Kinetic energy released on $F^- + NF_2$ as a function of the incident electron energy.

direct dissociation mechanism (see also below). The TOF doublet increases with electron energy at energies above ≈2.2 eV until an additional contribution between the doublet appears.

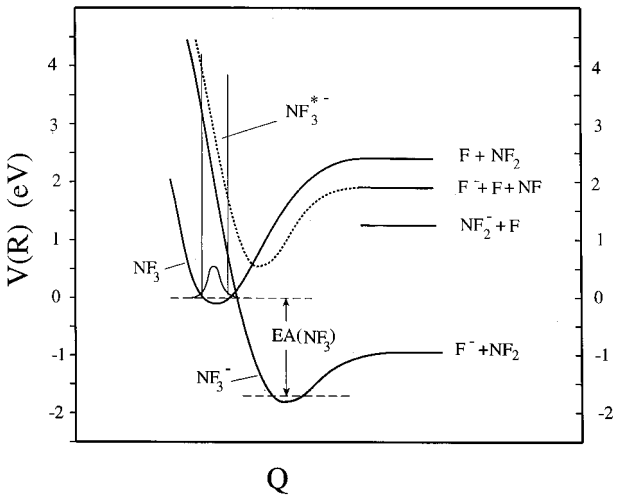

Figure 4. Schematic potential energy diagrams relevant for DA into $F^- + NF_2$. The adiabatic electron affinity $EA(NF_3) = 1.71$ eV is the result of the DFT calculation.

This contribution indicates F^- ions with low kinetic energy. They are most likely due to the multiple fragmentation process $F^- + F + NF$, which has an energetic threshold of 1.9 eV.[19] Note that the F^- yields in Figures 1 and 2 were recorded at different ion draw out fields, resulting in a different shape. Both curves, however, indicate that they consist of two overlapping resonances with maxima near 1.8 and 2.2 eV. The two other fragments (F_2^-, NF_2^-) in fact have relative cross sections peaking near 1.8 eV. We therefore suggest that two electronic states are involved: the electronic ground state of the anion at a vertical attachment energy near 1.8 eV and an electronically excited $NF_3{}^{*-}$ near 2.2 eV. The latter state decomposes into $F^- + F + NF$, yielding low-energy F^-. Since the TOF doublet still exists for electron energies above 3.5 eV, decomposition of $NF_3{}^{*-}$ into $F^- + NF_2$ cannot be excluded.

In Figure 3 the calculated translational energy imparted to $NF_2 + F^-$ as a function of the primary energy is plotted, yielding a straight line with a slope of 0.5. Figure 3 expresses that for "positive" electron energies 50% of it appears as an *increase* in the translational energy of the product. The ratio of the available excess energy ($\epsilon - \Delta H_o$) to the translational energy decreases with the electron energy ϵ. It is near 90% at $\epsilon = 0$. Such behavior was also reported for other *impulsive* DA reactions.[20,21]

The present situation can then be described in terms of a simplified one-dimensional potential energy diagram in Figure 4 with Q the relevant coordinate for the DA reactions of eq 1. Franck−Condon transitions between ≈0.5 and 3.5 eV create the transient negative ion in its electronic ground state, which above ≈2.2 eV overlaps with an electronically excited anion state. This second state is responsible for the structure in the F^- ion yield curve.

A closer inspection of the F^- relative cross section shows a small peak close to 0 eV below the low-energy tail of the resonant contribution. This "threshold" peak increases with the temperature of the target molecules, as can be seen from Figure 5. The appearance of such a threshold peak is a common feature in exothermic DA processes[22,23] when the potential energy of the curve crossing between the neutral and the ionic state is above the $v = 0$ vibrational level of the neutral molecule (see Figure 4).

The threshold signal then mirrors transitions from vibrationally excited states near the crossing point. Although the population of the relevant vibrational level may not be substantial, two effects contribute to the threshold intensity: (i)

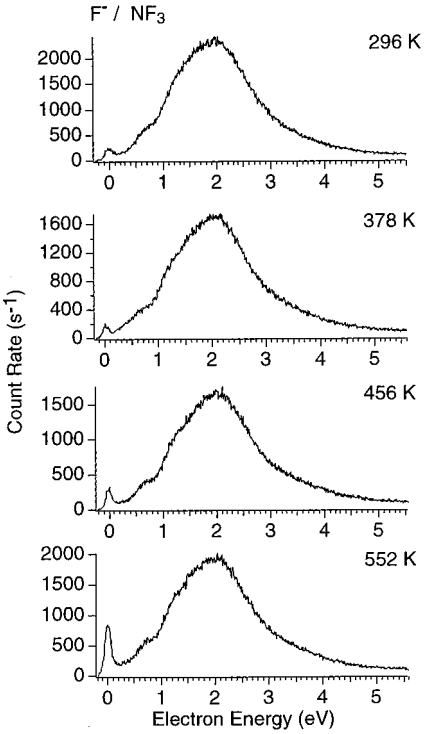

Figure 5. Dependence of the F^- channel from the temperature of the NF_3 molecules. The electron beam is adjusted to the threshold region (electron energy $\approx$ 0 eV).

transitions close to the crossing point have dissociation probabilities near unity (vanishing autodetachment) and (ii) the electron capture cross section behaves (apart from Franck−Condon factors) as $\sigma_o \approx \epsilon^{-1}$ or $\sigma_o \approx \epsilon^{-1/2}$ in the threshold region.[12,24] The potential energy of the crossing point can then be viewed as the activation energy E_a of the DA reaction for "zero-energy" electrons. The variation of the threshold signal with gas temperature in fact shows an Arrhenius-like behavior leading to $E_a = 0.1 \pm 0.05$ meV.

Flowing afterglow (FA) experiments, on the other hand, resulted in an activation energy of 300 ± 60 meV.[25] This value was obtained under "truly thermalized" conditions by varying the gas and electron temperature. As has recently been pointed out,[26] there exists principally a different influence of gas temperature and electron temperature on the (dissociative) attachment rate. It is, however, unlikely that this large discrepancy can be explained by this effect.

Since the attachment cross section increases toward low energies, the measured threshold intensity is very sensitive to the experimental conditions, i.e., to the energy resolution of the electron beam and the adjustment of the beam toward "zero" energy. On the other hand, the temperature dependence was recorded under exactly the same experimental conditions and reproduced several times so that the discrepancy of the FA result remains in question. Our DFT calculations predict an activation barrier *below* 0.2 eV (see below).

Free Electron Attachment to NF_3 Clusters. Figure 6 shows a negative ion mass spectrum obtained at an incident electron energy of 1.7 eV (which is close to the maxima in the DA cross sections). The cluster beam is established by expanding an NF_3/Ar gas mixture (1/50) at a pressure of 4 bar through the nozzle at room temperature. Apart from the DA fragments we observe "solvated" DA fragments of the form $F^-\cdot M_n$ ($M = NF_3$) and the homologous series M_n^- including the monomer NF_3^-, indicating that NF_3 possesses a positive (adiabatic) electron affinity and that the potential energy surface possesses a well-defined minimum. By variation of the stagnation pressure, the

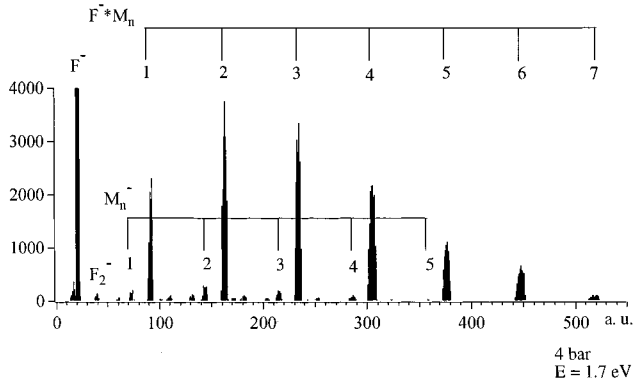

Figure 6. Negative ion mass spectrum obtained from free electron attachment to NF_3 clusters at an incident energy of 1.7 eV. The stagnation pressure is 4 bar.

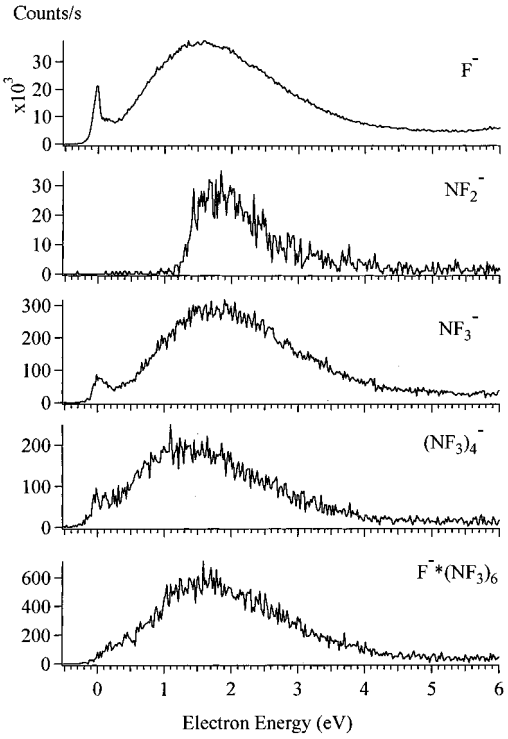

Figure 7. Relative cross section for some negative ions arising from free electron attachment to NF_3 clusters. The stagnation pressure is 4 bar.

type of observed product ions remains virtually unchanged. Only the mass distribution is shifted to larger compounds as the stagnation pressure increases, which reflects an increasing average size of the neutral cluster distribution in the beam. The same is true when a mass spectrum is recorded at an incident electron energy near 0 eV. The only difference concerns the fragments NF_2^- and F_2^-, which are absent near 0 eV for obvious reasons.

In Figure 7 we have plotted the explicit relative cross sections for a few product ions. It can be seen that the parent ion NF_3^- (and also the larger undissociated complexes $(NF_3)_n^-$) is still predominantly generated from the resonance around 2 eV. For NF_3^-, for example, this means that a relaxation energy of several electronvolts (amounting to $\epsilon + EA(NF_3)$) has to be carried off by the target cluster, ultimately leaving the naked monomer anion. Since this process is associated with a more or less complete evaporation of the target cluster, it is commonly assigned as *evaporative attachment.*[10] By the recording of larger ionic products, e.g., $(NF_3)_4^-$ or $F^-\cdot(NF_3)_6$ (Figure 7), the resonance maximum is somewhat shifted to lower energies. This

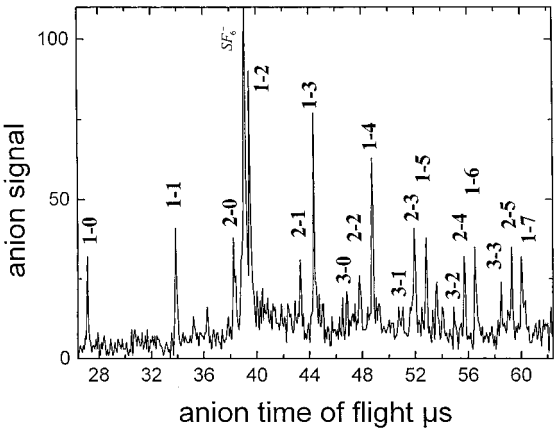

Figure 8. Negative ion mass spectrum obtained in RET to NF_3/Ar clusters. The numbers $n-m$ refer to $(NF_3)_n^-\cdot Ar_m$.

simply reflects the fact that these products result from larger target clusters with their larger polarizability and hence the larger solvation shift of the TNI formed in the initial step. The most remarkable feature, however, concerns a threshold peak that can be seen on those ionic products that arise from exothermic reactions. As mentioned above, the intensity of this threshold signal is very sensitive to the tuning of the electron beam toward very low energies.

In the isolated molecule the threshold peak in the F^- cross section was explained via Franck−Condon transitions from vibrationally excited neutrals close to the crossing point between the two relevant potential energy curves. In the supersonic beam the molecules in a cluster indeed have much less vibrational energy. On the other hand, the anionic curve is considerably lowered (solvation shift), which then makes "0 eV" transitions from the vibrational ground-state possible.

At this point it should also be emphasized that molecular clusters and large molecules (other than small targets) may gain the ability to trap electrons by a *direct coupling* of the incident electron with the many degrees of freedom rather than by the well-known *electronic resonance* mechanism. As mentioned above, for low energies the cross section behaves as $\epsilon^{-1/2}$ (Wigner theshold law[24]) or ϵ^{-1} ("s-wave" capture cross section[12]). Threshold attachment may be a quite general phenomenon in clusters. It has recently been demonstrated to be operative for clusters of O_2 [27] and O_3.[28] In both systems single molecules do not capture energy electrons near 0 eV.

Rydberg Electron Transfer (RET) to NF_3 Clusters and NF_3/Ar Clusters. In the RET experiment we also observe (as in the free electron experiment) ions of the form $(NF_3)_n^-$ and $F^-\cdot(NF_3)_n$ but also copious amounts of ions $NF_3^-\cdot Ar_n$. This is the result of the different expansion conditions creating more mixed neutral clusters rather than of the different electron energy.

In addition, by variation of the time delay between the opening of the pulsed valve and the laser firing, different beam conditions can be explored. At the early stage of the valve opening, the beam density is too low for cluster formation. Only dissociative attachment to the isolated NF_3 molecule is observed, in good agreement with the result of the free electrons. When the beam pressure increases, favoring beam clustering, one observes nondissociative attachment corresponding to the production of NF_3^-, as well as $(NF_3)_n^-$ and $NF_3^-\cdot Ar_n$ anions. As an example, a mass spectrum of homogeneous $(NF_3)_n^-$ and inhomogeneous $NF_3^-\cdot Ar_n$ cluster anions, obtained by collisions with Xe (n = 13, f) atoms, is displayed in Figure 8. The Rydberg atom principal quantum number n can be varied from

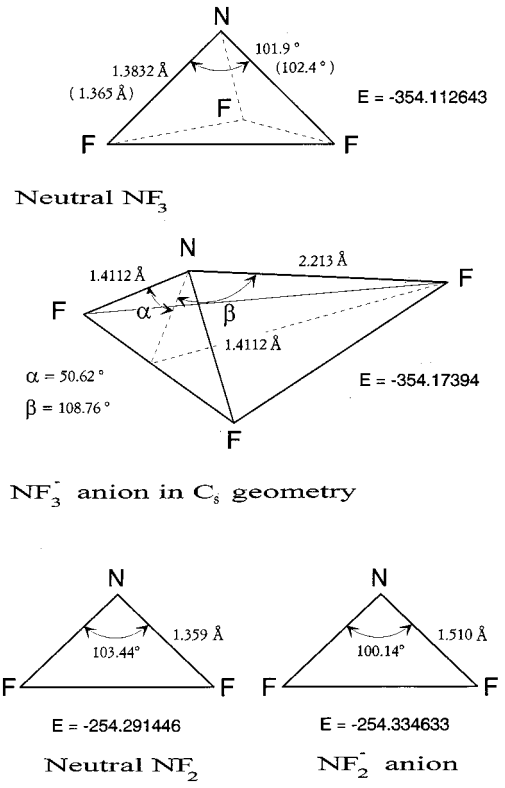

Figure 9. Calculated geometries for NF_3 and NF_2 and the corresponding relaxed anions.

7 to 50, corresponding to mean Rydberg electron energies between 280 and 5 meV. The n-dependencies of the rate constants for the formation of created anions are determined by comparison with SF_6^- signals due to collisions with a thermal effusive beam of SF_6 [16] and are typical of covalent anions (anions with excess electrons in valence orbitals). The dipole moment of NF_3 is 0.234 D, much smaller than the critical dipole moment of 2.5 D required to give birth to dipole-bound anions (anions with excess electrons in very diffusive orbitals located outside the molecular frame).[29,30]

Density Functional Theory Calculations. The observation of the NF_3^- anion in both free electron attachment (FEA) and Rydberg electron transfer (RET) measurements proves that the exit channels $NF_2^- + F$ and $NF_2 + F^-$ are endothermic with respect to the nondissociative attachment channel. We here wish to support this result by means of a quantum chemistry calculation. It is now known that the electronic structure of anions at least for large enough molecules can be obtained by means of the density functional theory (DFT).[30] We have used the Becke 3LYP functional containing the Slater exchange functional, Hartree−Fock and Becke's 1988 gradient correction,[31] combined with the Lee−Yang−Parr functional.[32] All calculations were made with the GAUSSIAN 92/DFT program.[33] The neutral NF_3 is a pyramid with C_{3v} symmetry. The anion exhibits a strong Jahn−Teller effect. With the C_{3v} geometry, the electron affinity is 1.15 eV and goes up to 1.71 eV in the C_s configuration (see Figure 9). The basis set is extracted from ref 34. It is not straightforward to calculate the energy of the transition state between NF_3 and NF_3^-. We have computed the respective energies in C_{3v} symmetry as a function of the N−F coordinate, resulting in $E_a = 0.2$ eV. Since this value is an overestimation (no relaxation of NF_3^-), we can conclude that DFT calculations predict an activation barrier below 0.2 eV, which would favor the value derived from the beam experiment (0.1 eV).

TABLE 1: Vibrational Frequencies in Neutral NF_3 in cm^{-1}

	ω_1	ω_2	ω_3[a]	ω_4[a]
DFT calcn	1028.5	640.4	870.9	481.3
exptl[36]	1032	647	907	492

[a] Doubly degenerate vibration.

TABLE 2: Calculated Frequencies of the NF_3^- Anion in cm^{-1}

ω_1	ω_2	ω_3	ω_4	ω_5	ω_6
97.3	144.3	300.4	506.4	782.0	935.2

The calculated electron affinity of the NF_2 radical is 1.18 eV, which is very close to that derived in the present DA experiment (1.1 ± 0.1 eV).

To further test the validity of these calculations, we compare the electronic properties of the neutral molecule with available experimental data in Table 1. Table 2 gives the calculated frequencies of the anion.

Conclusions

Electron capture by gas-phase NF_3 is purely dissociative and yields the ionic fragments F^-, F_2^-, and NF_2^- appearing from a broad resonance around 2 eV. From the vertical onset of the NF_2^- signal the adiabatic electron affinity for the corresponding radical is derived as $EA(NF_2) = 1.1 \pm 0.1$ eV, which is very close to the value from the present DFT calculations (1.18 eV).

From the temperature dependence of the F^- threshold signal (at "0" eV) the activation energy for the exothermic DA reaction $e^- + NF_3 \rightarrow NF_2 + F^-$ is derived as $E_a = 0.1 \pm 0.05$ eV. F^- appears from a pronounced *impulsive* dissociation process with 50% of the available energy released as kinetic energy of the two fragmentation products.

Both free electron attachment and Rydberg electron transfer (RET) generate ions of the form $F^-\cdot(NF_3)_n$ and $(NF_3)_n^-$ including the monomer NF_3^-. In the free electron experiment, the ions are still predominantly formed via the resonance around 2 eV.

Density functional theory (DFT) calculations predict the unrelaxed anion NF_3^- far from the geometry of the neutral with the C_{3v} symmetry lowered to C_s. The adiabatic electron affinity is calculated as $EA(NF_3) = 1.71$ eV.

Acknowledgment. The work was supported in part by the Deutsche Forschungsgemeinschaft and Fonds der Chemischen Industrie. S.M. thanks the Alexander von Humboldt-Stiftung for a research fellowship.

References and Notes

(1) Pellerite, M. J.; Brauman, J. I. *J. Am. Chem. Soc.* **1983**, *105*, 2672.
(2) Chantry, P. J. In *Applied Atomic Collision Physics*, Massey, H. S. W.; McDaniel, E. W., Bederson, B., Eds.; Academic Press: New York, 1982; Vol. 3.
(3) Bruno, G.; Capezzuto, P.; Cicala, G.; Manodoro, P. *J. Vac. Sci. Technol.* **1994**, *12*, 690.
(4) Greenberg, K. E.; Verdeyen, J. T. *J. Appl. Phys.* **1985**, *57*, 1596.
(5) Perrin, J.; Méot, J.; Siéfert, J. M.; Schmitt, J. *Plasma Chem. Plasma Process.* **1990**, *10*, 571.
(6) Harland, P. W.; Franklin, J. L. *J. Chem. Phys.* **1974**, *61*, 1621.
(7) Tides, G. D.; Tiernan, T. O. *J. Chem. Phys.* **1977**, *67*, 2382.
(8) Oster, T.; Kühn, A.; Illenberger, E. *Int. J. Mass Spectrom Ion. Processes* **1989**, *89*, 1.
(9) Ingólfsson, O.; Weik, F.; Illenberger, E. *Int. J. Mass Spectrom Ion Processes* **1996**, *155*, 1.
(10) Illenberger, E. *Chem. Rev.* **1992**, *92*, 1589.
(11) Stamatovic, A.; Schulz, G. J. *Rev. Sci. Instrum.* **1970**, *41*, 423.
(12) Klar, D.; Ruf, M.-W.; Hotop, H. *Aust. J. Phys.* **1992**, *45*, 263.
(13) Matejcik, S.; Kiendler, A.; Stamatovic, A.; Märk, T. D. *Int. J. Mass Spectrom. Ion Processes* **1995**, *149*/*150*, 311.
(14) Illenberger, E. *Chem. Phys. Lett.* **1981**, *80*, 153.
(15) Illenberger, E. *Ber. Bunsen-Ges. Phys. Chem.* **1982**, *86*, 252.
(16) Desfrançois, C.; Khelifa, N.; Lisfi, A.; Schermann, J. P. *J. Chem. Phys.* **1992**, *96*, 5009.
(17) Radzig, A. A.; Smirnov, B. M. *Reference Data on Atoms, Molecules and Ions*; Springer Series in Chemical Physics 44; Springer-Verlag: Berlin, 1985
(18) *JANAF Thermochemical Tables*, 3rd ed.; American Institute of Physics: New York, 1986.
(19) *Handbook of Chemistry and Physics*, 76th ed.; Lide, D. R., Ed.; CRC Press: Boca Raton, FL, 1995.
(20) Heni, M.; Illenberger, E. *Chem. Phys. Lett.* **1986**, *131*, 314.
(21) Illenberger, E.; Momigny, J. In *Gaseous Molecular Ions. An Introduction to Elementary Processes Induced by Ionization*; Baumgärtel, H., Franck, E. U., Grünbein, W., Eds.; Steinkopff-Verlag, Darmstadt/ Springer-Verlag: New York, 1992.
(22) Brüning, F.; Hahndorf, I.; Stamatovic, A.; Illenberger, E. *J. Phys. Chem.* **1996**, *100*, 14745.
(23) Hahndorf, I.; Illenberger, E. *Int. J. Mass Spectrom. Ion Processes*, in press.
(24) Wigner, E. P. *Phys. Rev.* **1948**, *73*, 1002.
(25) Miller, T. M.; Friedman, J. F.; Stevens Miller, A. E.; Pauson, J. F. *Int. J. Mass Spectrom. Ion Processes* **1995**, *149*/*150*, 111.
(26) Spanel, P.; Matejcik, S.; Smith, D. *J. Phys. B: At. Mol. Opt. Phys.* **1995**, *28*, 2941.
(27) Matejcik, S.; Kiendler, A.; Stampfli, P.; Stamatovic, A.; Märk, T. D. *Phys. Rev. Lett.* **1996**, *77*, 3771.
(28) Matejcik, S.; Cicman, P.; Kiendler, A.; Skalny, J. D.; Illenberger, E.; Märk, T. D. *Chem. Phys. Lett.* **1996**, *261*, 437.
(29) Desfrançcois, C.; Abdoul-Carine, H.; Schermann, J.-P. *Int. J. Mod. Phys.* **1996**, *10*, 1339.
(30) Rösch, N.; Trickey, S. B. *J. Chem. Phys.* **1997**, *106*, 8940.
(31) Becke, A. D. *J. Chem. Phys.* **1988**, *88*, 1053.
(32) Lee, C.; Wang, W.; Parr, R. G. *Phys. Rev. B* **1988**, *37*, 785.
(33) Frisch, M. J.; Trucks, G. W.; Schlegel, H. B.; Gill, P. M. W.; Johnson, B. G.; Wong, J. B.; Foresman, M. A.; Robb, M.; Head-Gordon, E. S.; Replogle, R.; Gomperts, R.; Andres, J. L.; Raghavachari, K.; Binckley, J. S.; Gonzalez, C.; Martin, R. L.; Fox, D. J.; Defrees, D. J.; Baker, J.; Steart, J. J. P.; Pople, J. A. *Gaussian 92/DFT*; Gaussian Inc.: Pittsburgh, 1993.
(34) Frisch, M. J.; Pople, J. A.; Brinckley, J. S. *J. Chem. Phys.* **1984**, *80*, 3265.